Food Hydrocolloids 147 (2024) 109341

Contents lists available at ScienceDirect

Food Hydrocolloids

journal homepage: www.elsevier.com/locate/foodhyd

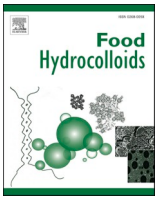

Conformational changes and product quality of high-moisture extrudates produced from soy, rice, and pea proteins

Boning Mao [a,b], Jaspreet Singh [a,b], Suzanne Hodgkinson [b], Mustafa Farouk [c], Lovedeep Kaur [a,b,*]

[a] School of Food and Advanced Technology, Massey University, 4442, Palmerston North, New Zealand
[b] Riddet Institute, Massey University, 4442, Palmerston North, New Zealand
[c] AgResearch Ltd., Ruakura Research Centre, Hamilton, New Zealand

ARTICLE INFO

Keywords:
Aggregates
High-moisture extrusion processing
Meat analogue
Protein secondary structure
Soy, pea, and rice proteins

ABSTRACT

This study aimed to investigate the performance of soy, pea, and rice proteins during high-moisture extrusion (HME) to understand better how the plant proteins transform into a fibrous structure. It found that rice protein isolate formed weak structures with the fewest layers and fibrous structures. Extruded pea protein concentrate produced more obviously layered structures than extruded soy and rice samples. Extruded soy protein isolate showed a compact gel structure, whereas extruded soy protein concentrate showed a thin fibrous structure. Meanwhile, the chewiness of soy and pea protein extrudates surpassed that of rice protein extrudates by approximately 10 N. After undergoing HME processing, there was a marked 5–10% decrease in extracted proteins ($p < 0.05$) in solvents with urea, dithiothreitol, and sodium dodecyl sulphate, when comparing the soy and pea extrudates with their raw materials, except for the extruded rice protein isolate (ERPI) with rice protein isolate. It could be deduced that HME processing promoted the formation of aggregates in soy and pea proteins that the extracted solvents could not dissolve. It also revealed that HME induced an increase in the content of S–S bonds in extruded soy and pea protein but a decrease in ERPI. The percentage of random coils in commercial pea protein, initially at 14.04%, saw a significant increase to 19.36% after extrusion ($p < 0.05$), indicating that pea protein is more likely to form intermolecular hydrogen bonds. In this study, the secondary structures of rice and soy protein did not show significant changes after extrusion.

1. Introduction

Plant-based meat analogues are gaining popularity because they are perceived as healthier and more sustainable alternatives to meat (Boukid, 2021; Choudhury, Singh, Seah, Yeo, & Tan, 2020). The market for plant-based meat is expected to grow to $85 billion in 2030 globally (Choudhury, et al., 2020; Singh et al., 2021). High-moisture extrusion (HME) is now the most widely used technique in the industry for preparing plant-based meat substitutes with meat-like fibrous structures and texture (Guyony, Fayolle, & Jury, 2022; Wittek, Karbstein, & Emin, 2021). The primary ingredient of plant-based meat substitutes is textured vegetable proteins (TVP), primarily made from soy, pea, peanut, and wheat (Baune, Terjung, Tülbek, & Boukid, 2022; Sasimaporn Samard, Maung, Gu, Kim, & Ryu, 2021; Zhang et al., 2019). Moreover, recent studies have also explored the potential use of other protein sources for plant-based meat analogues, such as rice (Lee, Oh, Choi, Yoon, & Han, 2022), mung bean (Branch & Maria, 2017), hemp (Zahari, et al., 2020) and potato (Boukid, 2021), among others.

The formation of fibrous structures in plant proteins via HME is currently being explained by two mainstream hypotheses (Beniwal, Singh, Kaur, Hardacre, & Singh, 2021; Van Der Sman & Van Der Goot, 2023). The first hypothesis proposes that the hydrated protein mix (60% water, 20% protein) is subjected to melting (or a "thermally plasticised" state) during extrusion at temperatures above 130 °C. Then fibre production occurs when protein aggregates are aligned under intense shear flow above denaturation temperatures (Akdogan, 1999). Another hypothesis considers that a blend with thermodynamically incompatible biopolymers, resulting in phase separation, is a prerequisite for a fibrous structure (Dekkers, Boom, & van der Goot, 2018; Tolstoguzov, 1993). Moreover, it is common to visualise a second polysaccharide phase by using confocal scanning laser microscopy of extrudates, where the protein and polysaccharide phases are marked differentially (Dekker et al., 2018). Additionally, other researchers have found that the soy-based meat analogues produced by HME were composed of a

* Corresponding author. School of Food and Advanced Technology, Massey University, 4442, Palmerston North, New Zealand.
E-mail address: L.Kaur@massey.ac.nz (L. Kaur).

https://doi.org/10.1016/j.foodhyd.2023.109341
Received 9 July 2023; Received in revised form 3 September 2023; Accepted 25 September 2023
Available online 25 September 2023

water-rich dispersed phase, surrounded by a water-poor continuous phase that has a higher concentration of protein (Wittek, et al., 2021). However, to thoroughly validate the hypotheses concerning the structuring of extruded meat analogues, multiple experimental methods are required for in-depth exploration.

Early studies on high-moisture extruded plant-based meats primarily used soy as the main component because of its superior gelation properties, allowing for the creation of a fibrous structure (Areas, 1992; He, Evans, Liu, & Shao, 2020). However, concerns about soy allergies and its predominant genetically modified nature have arisen (Rai et al., 2023; Sun, Ge, He, Gan, & Fang, 2021). Lately, peas are gaining popularity as a potential alternative to soy protein. Yet, products derived from peas tend to be softer and less elastic because of their limited gelling ability (Rai et al., 2023; Sun et al., 2021). Recognizing the nutritional and biological virtues of rice protein, recent innovations have resulted in the production of meat alternatives using both RPI and SPI via extrusion cooking (Lee, Choi, & Han, 2022; Lee, Oh, Choi, Yoon & Han, 2022b; Xiao et al., 2022). Combining 25%–100% (w/w) SPI with RPI enriches the product with methionine, an amino acid that is scarce in items made exclusively from SPI (Lee, Choi, & Han, 2022). Thus, in addition to soy and pea protein, rice protein was also chosen for this study to investigate the performance during HME.

The aims of this study were i) to investigate and draw correlations between the rheological properties of soy, pea, and rice proteins and the structure and textural attributes of their respective extrudates from a macroscopic view; ii) to delve into how High-Moisture Extrusion (HME) influences the interactions between plant protein molecules on a microscopic scale; iii) to analyse how thermo-mechanical processing during HME modifies the presence of disulphide bonds within the studied plant proteins; iv) to identify and detail alterations in the secondary structural formations of soy, pea, and rice proteins as a consequence of HME. Then, by harnessing the collected data, the purpose of this study was to gain a core comprehension of how plant proteins adapt and transform in response to thermo-mechanical actions during HME, setting a foundation for upcoming studies and progress in this area.

2. Materials and methods

2.1. Materials

Soy protein isolate (SPI, SUPRO 500E IP, 94% dry matter with 90% protein, 1% fat and 5% ash) was purchased from Solae (Winnipeg, USA); soy protein concentrate (SPC, Arcon SB, 90% dry matter with 65% protein, 4% fat and 7% ash) was purchased from Archer Daniels Midland Company, USA; pea protein concentrate (PPC, 92% dry matter with 76% protein, 1% fat and 8% ash) was purchased from Davis Food Ingredients (Palmerston North, New Zealand). Rice protein isolate (RPI, Remypro N80+, 92% dry matter with 83% protein, 5% fat and 2% ash) was purchased from Beneo Ibérica (Barcelona, Spain). The commercial plant protein powders used in this study had a moisture content ranging from 6-8%. All chemicals and reagents were of analytical grade.

2.2. High-moisture extrusion

The formulations subjected to extrusion are displayed in Table 1. A corotating, intermeshing twin-screw extruder on a pilot scale was used for all extrusion studies (Clextral BC-21, Firminy Cedex, France). Additionally, a long cylindrical cooling die with a 10/355 mm diameter was attached to the end of the extruder. The extrusion configurations were derived from the study by Chiang, Loveday, Hardacre, and Parker (2019) and Chiang et al. (2021). The barrel was divided into seven zones: the feeding zone (T1), six temperature-controlled zones (T2–T7) and a cooling zone (25 °C) that was maintained by pipes of running water. The barrel temperatures in the seven zones from the feed to the die were set to 20 °C, 50 °C, 80 °C, 110 °C, and 140 °C (for the last three zones), as we found that the minimum temperature to achieve

Table 1
The five formulations (powders) used for preparing meat analogues by high-moisture extrusion processing.

No.	Plant protein sources	Composition (% w/w)	Digital photos of the formulation
1	Pea protein concentrate (PPC) (76% protein content)	100	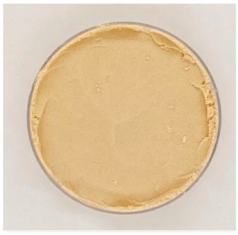
2	Soy protein concentrate (SPC) (65% protein content)	100	
3	Soy protein isolate (SPI) (90% protein content)	100	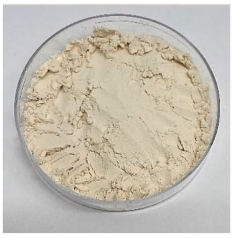
4	Rice protein isolate (RPI) (83% protein content)	100	
5	Combined plant protein formulation (PPF) (80% protein content)	70 PPI + 30 SPI	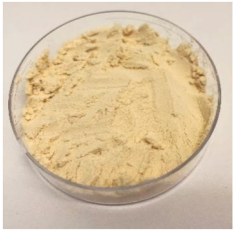

structured meat analogues was 140 °C according to the preliminary extrusion trails. The dry materials were fed into the extruder at 2.8 kg/h using a gravimetric feeder (K-ML-D5-KT20 and LWF D5, Coperion K-Tron, Switzerland). The screw speed was set to 400 rpm. A steady water supply at 3.6 kg/h was introduced into the extruder through an intake port to provide the finished product with a moisture content of roughly 60% w/w (wet basis). The extrudates were stored in plastic bags and frozen at −20 °*C* for future analysis.

2.3. Dynamic rheology

Dynamic rheological characterisation of the plant proteins was determined by using strain, temperature, and frequency sweeps, following the method of Wang, Kaur, Furuhata, Aoyama, and Singh (2022), with slight modifications. The rheological parameters, such as the storage modulus (G'), the loss modulus (G″) and tan δ, were recorded.

Based on the formula presented in Table 1, the commercial plant proteins were initially transformed into a paste with same moisture content of 25% (w/w). To achieve this, 200g of the dry powders were mixed with 600 mL of RO water using a kitchen mixer (KMM021, Kenwood, China) for a duration of 10 min. Post-mixing, this paste was stored in the refrigerator for 12 h to allow for uniform water dispersion. Prior to its rheometer assessment, the paste was allowed to sit at ambient temperature for 60 min to warm up. Visual representations of these plant protein pastes are available in Fig. S2 (Supplementary data). Then, the measurements of each formulation were prepared at the same moisture level (25%, w/w) and analysed for their rheological behaviour using a dynamic rheometer (AR-G2, TA Instruments, USA). A 40-mm parallel steel plate geometry was used with a gap of 2 mm between the plates. Data were collected and analysed by TA software (TA Universal Analysis Version 4.5A, TA Instrument, USA).

2.3.1. Temperature sweeps

Before the temperature and frequency sweeps, strain sweep measurements, within a range of 10^{-2}–10^{1} % strain, were performed to determine the linear viscoelastic region of the plant protein pastes at 25 °C and to ensure that the effects of mechanical stress on the structural changes were negligible. The strain sweep results are depicted in Fig. S1 (Supplementary Data). A strain value of 0.2% was chosen for the temperature and frequency sweep experiments, which was within the linear viscoelastic region of all the plant protein pastes.

A temperature sweep test aims to find how the viscoelastic properties of experimental samples change during heating and cooling. The samples were heated from 25 °C to 95 °C at a rate of 4 °C/min. After being held for 30 s at 95 °C, the samples were cooled from 95 °C to 25 °C at the same rate. At the end of the test, the cooled samples were held for 30 s at 25 °C. A small amount of mineral oil (Bio-Rad Laboratories, New Zealand) was applied to the sample edges to minimise water evaporation during the test (Wang, Kaur, et al., 2022).

2.3.2. Frequency sweeps

Oscillatory frequency sweeps were performed on the paste obtained after the temperature sweep experiments to check the strength of the gelation matrix of plant proteins. The oscillatory frequency sweeps were conducted at 25 °C, with the angular frequency increasing from 0.01 to 10 Hz.

2.4. Scanning electron microscopy

Scanning electron microscopy (SEM) is commonly applied to visualise the structures on the surface of meat analogues on a microscopic scale. The meat analogues were torn into pieces using tweezers measuring 10 mm × 10 mm × 10 mm and fixed into a solution of 2.5% glutaraldehyde in a 0.1 M phosphate buffer (pH 5.7) for at least 8 h at room temperature. After rinsing three times in a phosphate buffer solution (0.1M, pH 7.2), the samples were dehydrated in a graded series of ethanol solutions (25%, 50%, 75% and 95%) for 15 min each, with a final 100% ethanol wash for 1 h. Critical point drying was applied to the samples using liquid CO_2 and 100% ethanol. Once dried, the samples were mounted onto an aluminium stub using double-sided tape and silver conductive paint. Approximately 100 nm of gold (Baltec SCD 050 sputter coater) was sputter-coated into the surface of the samples, which were observed by (Quanta 200 Environmental, FEI Company, USA) at an accelerating voltage of 20 kV.

2.5. Colour measurement

A handheld chroma meter (CR 200, Konica Minolta, Tokyo, Japan) was used for measuring the colour of the meat analogues and plant protein powders. The instrument was first calibrated with a white tile. Colours were indicated by the CIE parameters as L* (0 = black and 100 = white), a* (greenness to redness) and b* (blueness or yellowness) (Holman, van de Ven, Mao, Coombs, & Hopkins, 2017). Six measurements were taken at random locations on the surface of the samples.

2.6. Textural properties

2.6.1. Cutting strength

The Warner–Bratzler shear force test was used to measure the force required to cut through a piece of each meat analogue as described by Chiang et al. (2021). The experiment was carried out on TA. XT Plus apparatus (Stable Micro Systems, UK). All plant-based extruded samples were cut into pieces measuring 40 mm × 15 mm × 5 mm (length × width × height). The samples were cut across the direction of the fibres at a speed of 2.00 mm/s using a V-notched blade with a 5-kg load cell and a trigger force of 0.049 N. The maximum force encountered during cutting was recorded for five repetitions.

2.6.2. Textural profile analysis

A texture profile analyser (TA.XT Plus, Stable Micro Systems, UK) was used to measure the hardness and chewiness as described by Chiang et al. (2021). The samples were cut into squares measuring 15 mm × 15 mm × 5 mm. A 50-kg load cell and a P/35 flat probe were used to achieve two compressions, which corresponded to the first and second bites, respectively. The probe returned to its original position after the first compression, which happened at a speed of 1 mm/s with a trigger force of 0.049 N until 50% of the original sample height was reached. The same parameters were used for the second compression until a further 50% reduction in the thickness of the first compressed layer was achieved.

2.7. Free sulfhydryl group content and disulphide bonds

The pre-conditioned Freeze Drier (Cuddon FD18, Blenheim, New Zealand) was loaded with frozen extrudates at a shelf temperature of –20 °C. Next, the condenser was adjusted to –40 °C. Upon reaching a vacuum level of around 1 mbar, the shelf temperature was raised to 20 °C to accelerate the sublimation process. The samples were then freeze-dried for about 72 h. After drying, the samples were ground with an electric bean grinder and filtered through an 80-mesh sieve. The content of free sulfhydryl groups (SH-free) and disulphide bonds (S–S bonds) in the raw materials and meat analogues were characterised as described by Xia et al. (2023). For this, 15 mg of powder was added to 5 mL of a Tris-glycine buffer. The buffer was made up of 0.086 M Tris, 0.09 M glycine, 0.04 M EDTA and 8 M urea. Next, 0.05 mL of Ellman's reagent (4 mg/mL) was added to the dispersion. The sample was then placed in the dark at 25 °C for 60 min, followed by being centrifuged at 5000×*g* for 5 min, and its absorbance was measured at 412 nm. The SH-free content (in μmol/g) was calculated according to Eq. (1),

$$\mathrm{SH-free} = \frac{73.53 \times \mathrm{A412} \times \mathrm{D}}{\mathrm{C}} \quad (1)$$

where D and C stand for the dilution factor and the protein concentration (mg/mL), respectively, and A412 is the absorbance at 412 nm.

Next, 1.5 mg of powder was added to 2.5 mL of the Tris-glycine buffer to measure the amount of S–S bonds in the extrudates and raw materials, then 25 mL of the reducing reagent β-mercaptoethanol was added to the dispersion. The sample was then kept in a water bath at 25 °C for 60 min. After thoroughly combining the dispersion with 5 mL of 12% trichloroacetic acid, it was centrifuged. The precipitate was washed with 5 mL of 12% trichloroacetic acid; then it was centrifuged. The protein was resuspended in 5 mL of the Tris-glycine buffer, and then 0.05 mL of Ellman's reagent was added. According to Equation (2), the S–S bonds (μmol/g) were calculated.

$$\text{S}-\text{S bonds} = \left(\frac{73.53 \times \text{A412} \times \text{D}}{\text{C}} - \text{SH}-\text{free}\right) \Big/ 2 \quad (2)$$

D and C are the dilution factor and protein concentration (mg/mL), respectively, and A412 is the absorbance at 412 nm.

2.8. Protein solubility

To evaluate the protein–protein interactions that occurred during HME, solutions extracted with specific reagents and their mixtures were used to analyse the protein interactions (Chiang et al., 2019; Lin et al., 2022). The buffers and their role in protein solubility are explained in Table S1 (Supplementary Data). In a centrifuge tube with 10 mL of each buffer system, samples weighing 0.2 g were extracted. After the mixture was shaken for 1 h in a water bath heated to 40 °C, it was centrifuged at 14,000×*g* for 15 min. The supernatant was then filtered with a 0.45-μm syringe filter. The protein in 2 mg/mL of bovine serum albumin (Sigma-Aldrich, USA) was used to create a standard curve. The soluble proteins in the supernatant were determined using the Bradford protein assay (Sigma-Aldrich, USA) at 595 nm with a spectrophotometer (SPECTRO star Nano, BMG LABTECH, Germany). The amount of soluble protein in the supernatant divided by the total protein in the samples was used to calculate the protein solubility. Each sample was measured three times. The Kjeldahl method was used to determine the total nitrogen in the original samples, and the protein content was determined using a conversion factor of 6.25 for all plant proteins.

2.9. Attenuated total reflectance – fourier transform infrared spectroscopy

The spectra of the freeze-dried powder samples were obtained using an attenuated total reflectance – Fourier transform infrared spectrometer (Nicolet 5700, Fisher Scientific, USA). Attenuated total reflection spectra were captured on a diamond crystal in 32 scans with a resolution of 4 cm^{-1}. According to Xia, Xue, Xue, Jiang, and Li (2022), the Amide I band (1700–1600 cm^{-1}) was used in the curve-fitting process to determine the secondary structures of the samples. The β-sheet band was reported to be located at 1613–1337 cm^{-1} and 1682–1696 cm^{-1}, the random coil band was reported to be at 1637–1645 cm^{-1}, the α-helix band was reported to be at 1645–1662 cm^{-1}, and the β-turn band was reported to be at 1662–1682 cm^{-1} and 1630 cm^{-1}.

Here, Omnic9.2 (Thermo Fisher Scientific Inc., MA, US) and Peakfit4.12 software (version 4.12, SPSS Inc., Chicago, IL, US) were used for baseline correction, smoothing and Fourier self-deconvolution. Fourier self-deconvolution and second-order derivative fitting were used to quantitatively analyse the second-order derivative of the Fourier transform infrared spectra.

2.10. Statistical analysis

Each experimental investigation had a minimum of three replicates for each measurement. Consequently, the data were presented as the means and standard deviation. The data were analysed with the statistical programme Minitab 21.3.1 (Minitab Inc. USA). Tukey's pairwise comparisons (at $p = 0.05$) and one-way analysis of variance were used to analyse the data at a 5% confidence level.

3. Results and discussion

3.1. Rheological properties of protein pastes

3.1.1. Temperature sweeps

Temperature sweeps were carried out to obtain information on the dynamic rheology properties of plant protein pastes prepared as described in Section 2.3, during heating and cooling situations. Fig. 1 depicts the rheological properties of the five paste formulations (25 wt %). The storage modulus G′ represents the elastic behaviour of the solid-like properties, whereas the loss modulus G″ relates to the viscosity of the polymer network. All plant protein pastes had a G′ higher than G″ within the linear viscoelastic range, indicating that the material behaved more like a solid (elastic deformation). The G′ and G″ of the control plant protein pastes decreased to a minimum during heating (G′ > G″), suggesting that heating can decrease the viscoelastic properties of hydrated plant protein dispersions. During cooling, the storage and the loss moduli of these samples increased continuously with a decrease in the

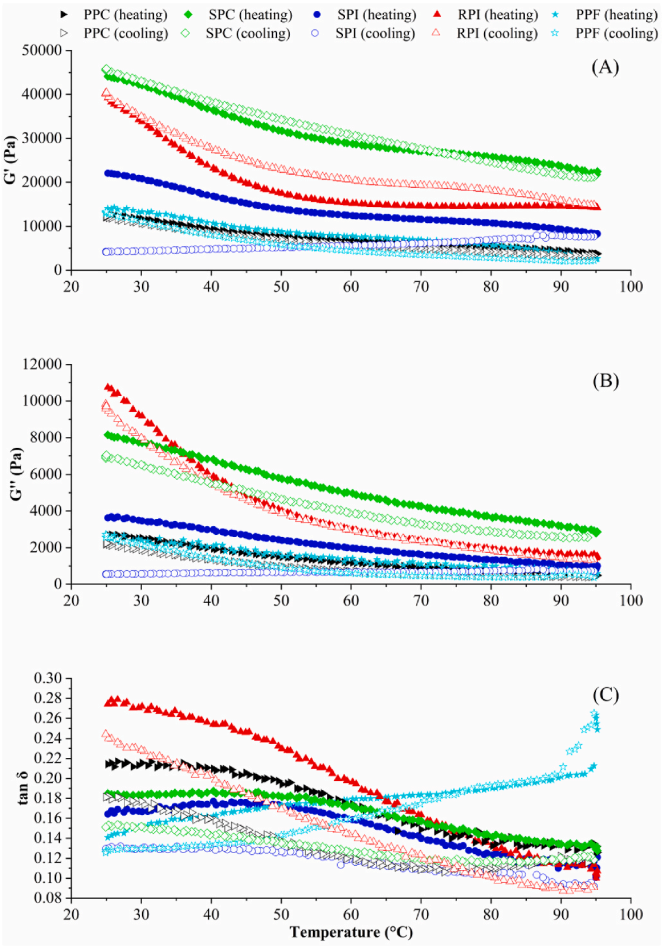

Fig. 1. Changes in the viscoelastic properties of plant protein pastes during temperature sweeps. Pea protein concentrate (PPC); Soy protein concentrate (SPC); Soy protein isolate (SPI); Rice protein isolate (RPI); Combined plant protein formulation (PPF). (A) Storage modulus (G′); (B) loss modulus (G″); (C) tan δ. Notes: All the tested plant protein pastes were prepared at the same moisture level (25% w/w). The samples were heated from 25 °C to 95 °C, then cooled back from 95 °C to 25 °C. The results shown were the mean value of triplicated tests.

temperature, except for the formulations containing SPI. No apparent changes in G′ and G″ values of SPI paste during the cooling stage. A possible explanation is that SPI can form a continuous, homogeneous phase during heating due to the lack of polysaccharides, resulting in low viscoelasticity properties during the cooling stage.

As tan δ describes the ratio of viscous to elastic behaviour, in Fig. 1C, the tan δ of all these samples mostly ranged between 0.1 and 0.25, indicating that the samples were always predominantly elastic. PPF paste, which had a mixture of two types of plant proteins, showed a completely different behaviour during heating and cooling than the pastes made up of single protein source. It had higher tan δ values than any of the single plant protein pastes at temperatures over 70 °C. This suggests that the paste made from both soy and pea proteins exhibited greater viscosity at high-temperature conditions. Apart from SPI, the G′ of the other four plant proteins remained relatively consistent from start to finish, although their G″ showed a decline by the end compared to the beginning. This resulted in a decrease in tan δ at the end of cooling in the plant protein pastes. In the case of SPI, both G′ and G″ saw a reduction, yet its tan δ also diminished. At the end of cooling, the tan δ value for all plant protein pastes ranked as follows: SPI ≈ PPF < SPC < PPC < RPI. This suggests that the cooled pastes from SPI and SPC had greater elasticity and reduced viscosity compared to the other mixtures. This finding is in agreement with that the meat analogues produced from soy proteins showed a higher value of chewiness, see Fig. 4.

3.1.2. Frequency sweeps

The results of the frequency sweep experiments with the frequency increasing from 0.01 to 10 Hz are shown in Fig. 2. All the extruded samples were predominantly elastic, with G′>G″, implying the typical characteristics of cross-linked networks with a gel-like behaviour. G′ and G″ increased gradually with an increase in the frequency, which may have been caused by the disentanglement of the molecular chains during the short period of oscillation. The G′ values were observed to increase in the order SPC > RPI > PPF ≈ PPC > SPI during the frequency sweep (Fig. 2A). There was a positive correlation between the value of G′ and hardness. These findings may indicate that the higher elastic properties resulted in greater structural strength in terms of hardness and chewiness. Furthermore, the lower the tan δ at a given frequency, the stronger the gel formed (Wittek et al., 2021; Yuliarti, Kiat Kovis, & Yi, 2021). This finding is consistent with the textural properties of the extrudates, as discussed in Section 3.4. It can also be deduced that soy and pea proteins could form robust structures, whereas rice protein form weak structures (Fig. 3).

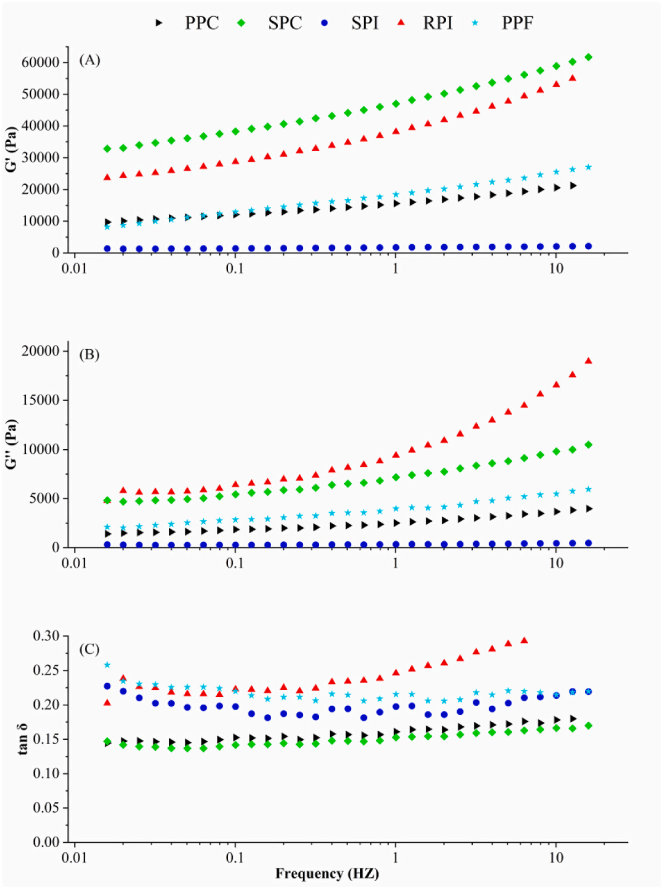

Fig. 2. Changes in the viscoelastic properties of plant protein pastes during frequency sweeps (from 0.01 to 10 Hz). Pea protein concentrate (PPC); Soy protein concentrate (SPC); Soy protein isolate (SPI); Rice protein isolate (RPI); Combined plant protein formulation (PPF). (A) Storage modulus (G′); (B) loss modulus (G″); (C) tan δ. Notes: All the tested plant protein pastes were prepared at the same moisture level (25% w/w). The results shown were the mean value of triplicated tests.

3.2. Product colour

Table 2 lists the colour parameters of the raw materials and extruded samples. Compared with the raw materials of PPC and RPI, the ingredients of SPC and SPI had much greater L* but lower b* values. Extrusion processing had a significant ($p < 0.05$) impact on the colour characteristics of the extrudates. All the extrudates showed a decrease in the L* and b* values but an increase in the a* value compared with their corresponding raw ingredients. These results indicated that the extrusion processing can reduce the brightness and whiteness of plant protein materials. PPC was more susceptible to an increase in redness during extrusion, showing a notable increase in the a* value from 1.81 to 3.66.

Previous studies reported that changes in the colour during the extrusion process mainly resulted from the Maillard reaction and caramelisation (Lee, Oh, Choi, Yoon & Han, 2022; Ma, Jin, Wang, & Tian, 2022; Wang et al., 2022). It is suspected that during thermomechanical processing, starch and sucrose might be hydrolysed into reducing sugars, which contribute to the production of caramel colours. This could explain the increase in the a* value (greenness to redness) and the decrease in the L* value (black to white) in extrudate samples compared with the raw materials. However, because of the different protein sources and the absence of myoglobin, the colour of texturized vegetable protein differed noticeably from that of all cooked meats. Compared with cooked beef and pork, the meat analogues produced by HME displayed less redness and darkness (Samard & Ryu, 2019).

3.3. Visual surface and microstructures of meat analogues

Fig. 3 depicts the visual surface and the inner structure of the longitudinal surface of the extrudates. The EPPC and EPPF showed a distinct layered structure along the extrusion direction but looked different. EPPC had an overall fine and tightly layered structure. The layered structure became more stretched and compact in the EPPF compared with the EPPC. This indicated that adding SPI to the formulation was beneficial for generating a more compact structure. The exterior surface of ERPI became coarser, and its internal composition displayed vague layers and fragile and loose structure. Additionally, it was observed that SPI extrudates showed a compact and gel structure with fewer layers and a less fibrous structure, which was consistent with the results of previous studies (Grabowska, Tekidou, Boom, & van der Goot, 2014; Meng, Chen, Zhao, Wei, & Zhang, 2022). Compared with ESPI, ESPC had a more apparent fibrous structure because of the two separate phases of protein and starch in the SPC.

Further analyses using SEM were carried out to obtain more detailed information on the protein network structure of the meat analogues, as illustrated in Fig. 3. The EPPC showed a thick lamellar structure. In contrast, the EPPF exhibited a clear, thin laminar structure. Apparent layers and an interconnected microstructure were obtained in the EPPF.

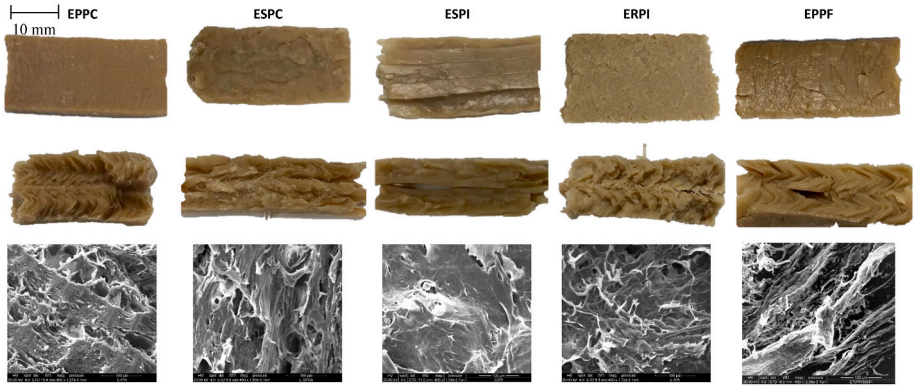

Fig. 3. Visual images and the microstructure of the plant protein extrudates were obtained by a scanning electron microscope (10,000 ×). Extruded pea protein concentrate (EPPC); Extruded Soy protein concentrate (ESPC); Extruded Soy protein isolate (ESPI); Extruded Rice protein isolate (ERPI); Extruded Combined plant protein formulation (EPPF).

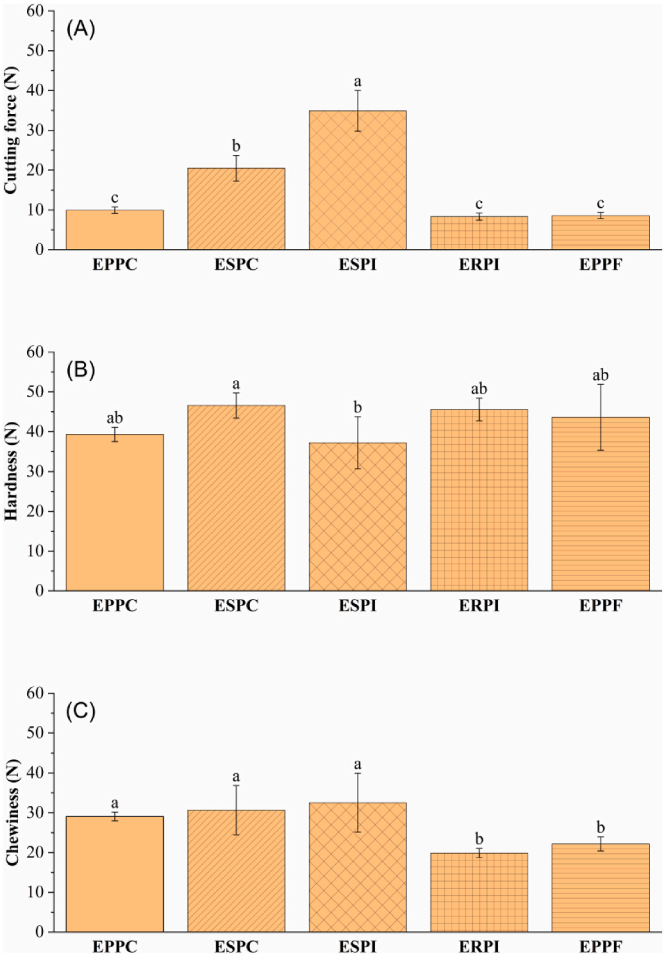

Fig. 4. The textural properties of the extrudates. Extruded pea protein concentrate (EPPC); Extruded Soy protein concentrate (ESPC); Extruded Soy protein isolate (ESPI); Extruded Rice protein isolate (ERPI); Extruded Combined plant protein formulation (EPPF). (A) Cutting force; (B) hardness; (C) chewiness. Notes: Data represent the mean and standard deviation. Different lowercase letters in the same graph indicate significant differences ($P < 0.05$).

ESPC showed a thin fibrous structure. For SEM imaging, the extrudates were torn into tiny fragments. The broken surface of the ESPI looked smooth and devoid of obvious layers, aligning with the observation that it predominantly appears gel-like shown in its digital images. Even though the torn ERPI did not show clear lamellae or fibre-like structures,

Table 2
L*, a* and b* colour parameters of the raw protein powders and their extrudates.

Sample	Treatments	colour		
		L*	a*	b*
PPC	Raw	87.32 ± 0.40^{c}	1.81 ± 0.02^{bc}	23.46 ± 0.01^{a}
	HME	62.57 ± 0.45^{e}	3.66 ± 0.33^{a}	16.43 ± 0.38^{b}
SPC	Raw	91.53 ± 0.19^{a}	1.04 ± 0.01^{de}	14.46 ± 0.09^{cd}
	HME	62.44 ± 1.13^{e}	1.31 ± 0.11^{d}	13.04 ± 0.44^{e}
SPI	Raw	91.95 ± 0.74^{a}	0.08 ± 0.02^{g}	14.16 ± 0.02^{d}
	HME	59.05 ± 1.57^{f}	0.75 ± 0.12^{ef}	12.06 ± 0.54^{f}
RPI	Raw	88.21 ± 0.18^{bc}	0.65 ± 0.02^{f}	16.73 ± 0.19^{b}
	HME	68.89 ± 0.79^{d}	1.68 ± 0.27^{c}	16.54 ± 0.16^{b}
PPF	Raw	89.09 ± 0.08^{b}	1.26 ± 0.03^{d}	16.73 ± 0.28^{b}
	HME	63.45 ± 0.63^{e}	2.04 ± 0.20^{b}	14.99 ± 0.36^{c}

Note: Data represent the mean and standard deviation. Different lowercase letters in the same column indicate significant differences ($P < 0.05$). Pea protein concentrate (PPC); Soy protein concentrate (SPC); Soy protein isolate (SPI); Rice protein isolate (RPI); Combined plant protein formulation (PPF); High-moisture extrusion (HME).

it exhibited uneven ruptures. This implies that the ERPI has a more fragile and uneven structure. These observations agree with their visual images. According to the dynamic rheology study (Section 3.1), the pastes of the combined plant protein formula (PPF) had the highest viscoelasticity (tan δ) at 95 °*C* of the temperature sweeps. Meantime, the value of tan δ gradually decreased during cooling. It could be deduced that the hot melted PPF passing through the cooling die had a higher flow rate and generated more obvious viscosity gradients than the other formulations, indicating that PPF could easily form lamellar structures. By contrast, SPI showed the lowest viscoelasticity at 95 °*C* and no apparent significant change in the value of tan δ during the cooling stage of the temperature sweep, resulting in ESPI showing a compact gel structure with a less apparent lamellar structure.

3.4. Textural characteristics

The transversal cutting strength, hardness, and chewiness of the extrudates are displayed in Fig. 4. More textural profile results are displayed in Table S1 (Supplementary Data). The ESPI and ESPC had significantly ($p < 0.05$) higher transversal cutting strengths than the other three formulations (Fig. 2A). This result confirmed that soy proteins were beneficial for generating a hard texture in meat analogues, compared with pea and rice protein products.

Hardness refers to the force needed to achieve a given deformation. ESPI had the lowest hardness value (Fig. 4B), which is consistent with the lowest value of G′ in the frequency sweep (Fig. 2C), indicating that the SPI formed a more resilient gel structure. Chewiness refers to the

amount of energy required to chew solid food until it's prepared to be swallowed. As shown in Fig. 4C, extruded pea and soy proteins displayed a significant ($p < 0.05$) higher chewiness than ERPI, which is in agreement with the paste of RPI showing the highest value of tan δ in the frequency sweep, indicating that rice protein formed weaker structure by HME. Additionally, the diminished chewiness value of ERPI aligns with its less defined layers and a looser texture. On the other hand, extruded pea and soy proteins exhibit a more rigid, gel-like structure (Fig. 3), which corresponds to their higher chewiness.

During commercial manufacturing, RPI is extracted from rice flour using alkaline methods, primarily isolating the protein known as the glutelin fraction, which possesses low water absorption and gelation abilities (Omura et al., 2021). Consequently, RPI struggled to form cross-linked 3D gel structures during HME pressing processes (Fig. 3). This leads ERPI to have more ambiguous layering, a softer texture with lowest cutting force and chewiness (Fig. 4A&C). Besides, the chewiness values for EPPC, ESPC, and ESPI were roughly 30 N, comparable to the value of cooked chicken breast at 28 N, as reported by Samard and Ryu (2019).

3.5. Protein solubility

The protein–protein interactions of the raw materials and extrudates were determined by a protein solubility study, as described by Chiang et al. (2019). It was reported that only protein molecules in their native states could be dissolved in the phosphate buffer. According to the data, the phosphate buffer extracted the least amount of protein from the raw plant protein powder and extrudates, between 0.65 and 5.36% (Fig. 5). This outcome was probably caused by the commercial pea, soy, and rice protein, which had undergone heat treatment, resulting in denaturation during manufacture. In particular, the extractable protein from all extrudates decreased in the phosphate buffer after HME compared with the raw materials, indicating that the extrusion process promoted the formation of aggregates.

The proteins in all samples became more soluble when the phosphate buffer and reagents (urea, dithiothreitol (DTT) or sodium dodecyl sulphate (SDS) were combined, indicating that the proteins in the raw sample and the extrudates were formed through a variety of chemical interactions (Fig. 5). Notably, the amount of protein solubilised by the phosphate buffer–urea was the highest of the two-component solvents, indicating that a significant amount of the protein in pea, soy and rice

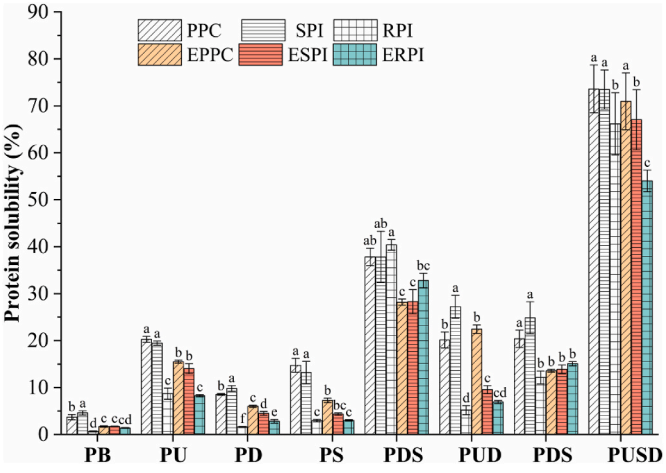

Fig. 5. Percentage of protein in the plant protein and their extrudates extracted by different solvents. P: 0.1 M phosphate buffer consisting of KH2PO4 and K2HPO4 with a pH of 7.5. PU: 8 M Urea (U) in P; PD: 0.05 M dithiothreitol (D) in P; PS: 1.5 g/100 ml sodium dodecyl sulphate (S) in P; PUD: 8 M Urea +0.05 M DTT in P; Raw plant protein materials: Pea protein concentrate (PPC); Soy protein isolate (SPI); Rice protein isolate (RPI); Extrudates (E). Note: Data represent the mean and standard deviation. Different lowercase letters in the same column indicate significant differences ($P < 0.05$).

was linked by hydrogen bonds. The lower amount of protein soluble in the phosphate buffer–SDS and phosphate buffer–DTT solvents revealed that disulphide bonds and hydrophobic interactions were not as significant. These results suggested that hydrogen bonds were the major force in the formation and stabilisation of the structure of meat analogues.

When two or more reagents were combined with the phosphate buffer, the protein solubilisation increased further (Fig. 5). Firstly, protein solubility was highest for all samples in the phosphate buffer–urea–DTT solvent, compared with the sum of the phosphate buffer–urea and phosphate buffer–DTT solvents. This could be a result of the synergistic effect of the two reagents. A similar synergy between urea and DTT has been reported (Chiang, et al., 2019; Lin et al., 2022). A possible explanation is that some of the tertiary and quaternary structures formed by non-covalent interactions were disrupted by urea, and the disulphide bonds inside them became exposed and were more easily reduced by DTT. By contrast, the protein solubilised by a combination of the phosphate buffer–DTT–SDS solvent (disulphide bonds and hydrophobic interactions) was approximately equal to the sum of the phosphate buffer–DTT and the phosphate buffer–DTT and the phosphate buffer–SDS solvents, and the same was true for the phosphate buffer–urea–SDS solvent vs the phosphate buffer–urea and the phosphate buffer–SDs solvents (Fig. 5).

The percentage of proteins extracted dropped significantly in the solvents after extrusion. This could be explained by that the extracted solvents could not dissolve the protein aggregations formed during extrusion. However, an interesting finding is that the protein solubility of ERPI in PD was higher than that in the raw rice protein sample, which agrees with the results in Section 3.6. This finding suggests that the HME process induced the new S–S bonds in the soy and pea proteins, but HME broke the initial S–S bonds in the rice protein.

3.6. Free sulfhydryl groups and disulphide bonds

Fig. 6 shows the content of SH-free and S–S bonds in the raw materials and extrudates. The content of SH-free in the raw PPC, SPC, SPI and PPF decreased significantly ($p < 0.05$) after extrusion, whereas there was no significant change in the raw RPI (0.34 μmol/g) and ERPI (0.42 μmol/g). The amount of SH-free in raw PPI was 6.19 μmol/g, which then decreased to 1.70 μmol/g after extrusion. The samples of SPC and SPI revealed a comparable decline, from 3.6 μmol/g in the raw materials to 0.7 μmol/g in the extrudates (Fig. 6A). It is possible to conclude that HME may cause the free sulfhydryl groups in soy and pea protein to oxidise.

In Fig. 6B, the results showed that raw RPI had the highest amount of S–S bonds (6.33 μmol/g), but the S–S bonds could be broken down by the extrusion process, decreasing to 2.2 μmol/g. Unlike RPI, the content of the S–S bonds in PPC, SPC, SPI and PPF experienced an increase after the extrusion process. The results indicated that PPC is more likely to form S–S bonds during extrusion, as these increased by 4 μmol/g. Branch and Maria (2017) reported an increase in the S–S bond content with a decrease in SH-free in texturized mung bean protein. This study also found similar results for the pea and soy protein extrudates but not rice protein. The results indicated that the free sulfhydryl groups inside soy and pea protein were oxidized and formed disulphide bonds, whereas the natural disulphide bonds of rice protein were broken during HME.

3.7. Secondary structures of proteins

Fig. 7 displays the ratios of the secondary structures of proteins between the raw materials and their extrudates. Soy, pea, and rice proteins predominantly contain β-sheets, which aligns with the findings presented in Shevkani, Singh, Chen, Kaur, and Yu (2019). It has been reported that the α-helix and β-sheet structures are tight and ordered structures, whereas β-turn and random coil structures are loose and disordered structures (Xiao, et al., 2022). It has also been reported that α-helixes and β-sheets are maintained by intramolecular hydrogen bonds.

As presented in Fig. 7, the pea protein contained the most ordered

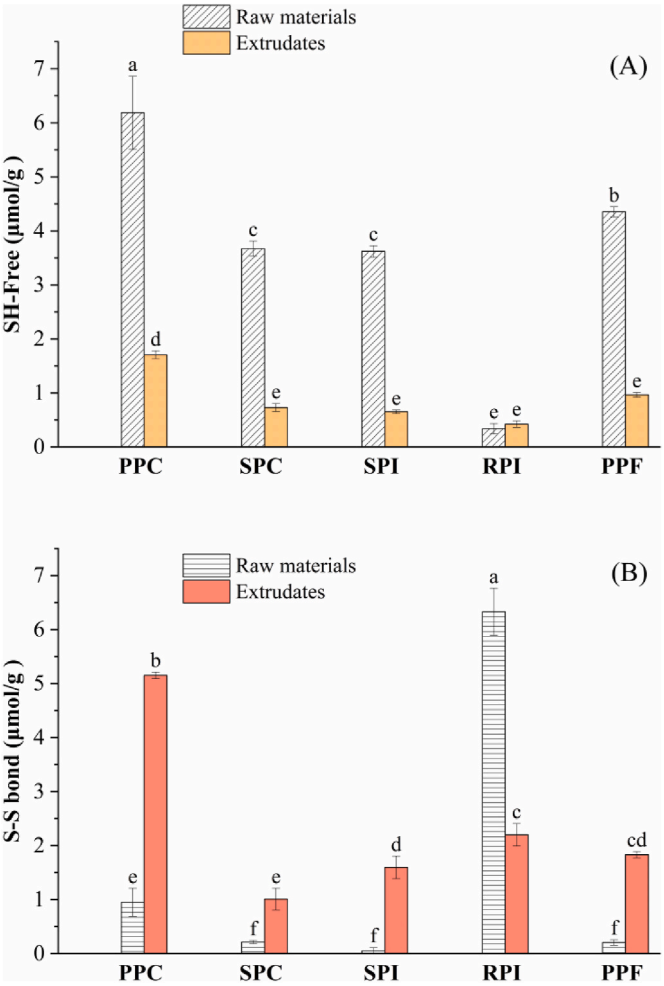

Fig. 6. The contents of the SH-free group (A) and S–S bond (B) in the raw materials and their extrudates. Raw plant protein materials: Pea protein concentrate (PPC); Soy protein concentrate (SPC); Soy protein isolate (SPI); Rice protein isolate (RPI); Combined plant protein formulation (PPF). Note: Data represent the mean and standard deviation. Different lowercase letters in the same column indicate significant differences ($P < 0.05$).

structures (α-helix and β-sheet) (67%). However, the ordered structures in pea protein were more susceptible to being affected by extrusion processing and transformed into disordered structures. While rice protein also showed a decline in its ordered structure after extrusion, the change was not significant ($p > 0.05$). Meanwhile, the ordered structure in soy proteins remained stable before and after HME processing. This indicated that the intramolecular hydrogen bonds in pea protein were more vulnerable to disruption by HME processing compared to those in rice and soy proteins.

Strong intermolecular hydrogen bonds maintain β-turns. The content of β-turns also indicates cross-linking and the formation of intermolecular aggregates (Xiao, et al., 2022; Zhang, Kang, Cheng, Cui, & Abd El-Aty, 2022). Random coils are maintained by the intermolecular hydrogen bonds formed between C═O and H_2O (Gao, Sun, Zhang, Sun, & Jin, 2022).

The results suggested that thermomechanical processing could cause intramolecular hydrogen bonds to change to intermolecular hydrogen bonds, as all the content of random coils in raw materials increased after extrusion. In particular, the number of random coils in PPC increased significantly ($p < 0.05$) after extrusion, indicating that pea protein was more likely to form intermolecular hydrogen bonds. This finding was consistent with the report by Wang, Kaur, et al. (2022), who found that the water in PPI extrudates migrate more easily compared with the

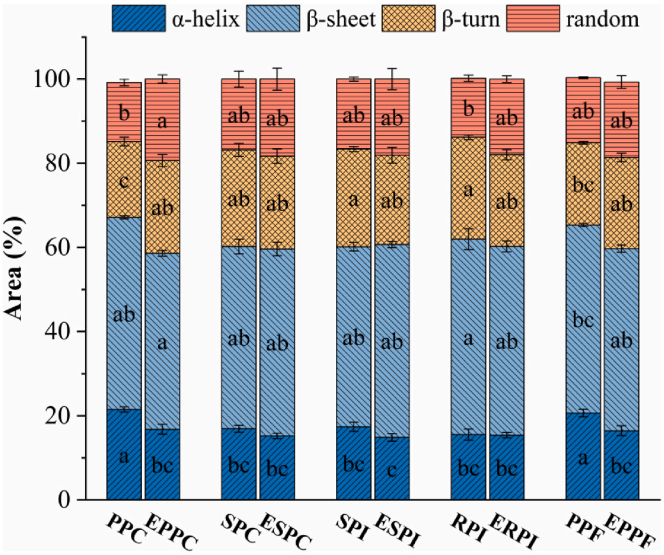

Fig. 7. Changes in the relative proportion of the secondary structures of plant proteins after high-moisture extrusion. Pea protein concentrate (PPC); Soy protein concentrate (SPC); Soy protein isolate (SPI); Rice protein isolate (RPI); Combined plant protein formulation (PPF); Extrudates (E). Note: Data represent the mean and standard deviation. Different lowercase letters in the same category indicate significant differences ($P < 0.05$).

counterpart in SPI, according to an investigation of the moisture distribution in meat analogues by low-field nuclear magnetic resonance. In rice protein, there was a decrease in β-sheet and β-turn structures while random coils saw an increase. This suggests that during HME, the intermolecular and strong intermolecular hydrogen bonds were disrupted, leading to the formation of new intermolecular hydrogen bonds.

4. Conclusions

To better understand the performance of soy, pea and rice proteins subjected to the same HME processing conditions, this study compared the physicochemical properties of high-moisture extrudates prepared from these plant proteins and their dynamic rheological properties. Furthermore, the lower the tan δ at a given frequency, the stronger the gel formed. As the protein paste made from soy and pea has lower tan δ in the frequency sweeps. The protein paste derived from soy and pea displayed a lower tan δ during frequency sweeps. This implies that soy and pea proteins can establish a stronger structure, while rice proteins develop a more fragile structure when subjected to heating and cooling processes. This finding was consistent with the textural properties; the extruded samples from soy and pea protein showed greater structural strength in terms of chewiness. HME processing promoted the formation of aggregates in plant proteins. However, the initial S–S bonds in rice protein could be broken by HME. The secondary structures of rice and soy protein did not show significant changes after extrusion. In contrast, the ordered structures in pea protein were more susceptible to being affected by the extrusion process and transformed into disordered structures.

Based on the performance of soy, pea and rice protein extrudates, this study provides thorough information for researchers and the industry to help them choose raw protein ingredients for high-moisture plant-based meat analogues. Moreover, our work contributes to a better comprehension of the mechanisms underlying fibre development in HME.

Author contribution statements

Lovedeep Kaur: Conceptualization, Supervision, Methodology, Writing- Reviewing and Editing. Jaspreet Singh: Conceptualization,

Methodology, Writing-Review and Editing, Supervision. Suzanne Hodgkinson: Writing-Review and Editing, Supervision. Mustafa Farouk: Writing-Review and Editing, Supervision. Boning Mao: Conceptualization, Formal analysis, Investigation, Data Curation, Writing-Original Draft.

Declaration of competing interest

The authors have no conflict of interest to declare.

Data availability

Data will be made available on request.

Acknowledgements

We are grateful to the AgMARDT (NZ) and Riddet Institute (NZ) for funding this research. The authors thank Chris Hall for his help with the extrusion experiment and Dr Yanyu He for her assistance with the SEM analysis.

Appendix A. Supplementary data

Supplementary data to this article can be found online at https://doi.org/10.1016/j.foodhyd.2023.109341.

References

Akdogan, H. (1999). High moisture food extrusion. *International Journal of Food Science and Technology, 34*(3), 195–207. https://doi.org/10.1046/j.1365-2621.1999.00256.x

Areas, J. A. (1992). Extrusion of food proteins. *Critical Reviews in Food Science and Nutrition, 32*(4), 365–392. https://doi.org/10.1080/10408399209527604

Baune, M.-C., Terjung, N., Tülbek, M.Ç., & Boukid, F. (2022). Textured vegetable proteins (TVP): Future foods standing on their merits as meat alternatives. *Future Foods, 6*, Article 100181. https://doi.org/10.1016/j.fufo.2022.100181

Beniwal, A. S., Singh, J., Kaur, L., Hardacre, A., & Singh, H. (2021). Meat analogs: Protein restructuring during thermomechanical processing. *Comprehensive Reviews in Food Science and Food Safety, 20*(2), 1221–1249. https://doi.org/10.1111/1541-4337.12721

Boukid, F. (2021). Plant-based meat analogues: From niche to mainstream. *European Food Research and Technology, 247*(2), 297–308. https://doi.org/10.1007/s00217-020-03630-9

Branch, S., & Maria, S. (2017). Evaluation of the functional properties of mung bean protein isolate for development of textured vegetable protein. *International Food Research Journal, 24*(4), 1595–1605.

Chiang, J. H., Loveday, S. M., Hardacre, A. K., & Parker, M. E. (2019). Effects of soy protein to wheat gluten ratio on the physicochemical properties of extruded meat analogues. *Food Structure, 19*. https://doi.org/10.1016/j.foostr.2018.11.002

Chiang, J. H., Tay, W., Ong, D. S. M., Liebl, D., Ng, C. P., & Henry, C. J. (2021). Physicochemical, textural and structural characteristics of wheat gluten-soy protein composited meat analogues prepared with the mechanical elongation method. *Food Structure, 28*. https://doi.org/10.1016/j.foostr.2021.100183

Choudhury, D., Singh, S., Seah, J. S. H., Yeo, D. C. L., & Tan, L. P. (2020). Commercialization of plant-based meat alternatives. *Trends in Plant Science, 25*(11), 1055–1058. https://doi.org/10.1016/j.tplants.2020.08.006

Dekkers, B. L., Boom, R. M., & van der Goot, A. J. (2018). Structuring processes for meat analogues. *Trends in Food Science & Technology, 81*, 25–36. https://doi.org/10.1016/j.tifs.2018.08.011

Gao, Y., Sun, Y., Zhang, Y., Sun, Y., & Jin, T. (2022). Extrusion modification: Effect of extrusion on the functional properties and structure of rice protein. *Processes, 10*(9). https://doi.org/10.3390/pr10091871

Grabowska, K. J., Tekidou, S., Boom, R. M., & van der Goot, A. J. (2014). Shear structuring as a new method to make anisotropic structures from soy-gluten blends. *Food Research International, 64*, 743–751. https://doi.org/10.1016/j.foodres.2014.08.010

Guyony, V., Fayolle, F., & Jury, V. (2022). High moisture extrusion of vegetable proteins for making fibrous meat analogs: A review. *Food Reviews International, 1–26*. https://doi.org/10.1080/87559129.2021.2023816

He, J., Evans, N. M., Liu, H., & Shao, S. (2020). A review of research on plant-based meat alternatives: Driving forces, history, manufacturing, and consumer attitudes. *Comprehensive Reviews in Food Science and Food Safety, 19*(5), 2639–2656. https://doi.org/10.1111/1541-4337.12610

Holman, B. W., van de Ven, R. J., Mao, Y., Coombs, C. E., & Hopkins, D. L. (2017). Using instrumental (CIE and reflectance) measures to predict consumers' acceptance of beef colour. *Meat Science, 127*, 57–62. https://doi.org/10.1016/j.meatsci.2017.01.005

Lee, J.-S., Choi, I., & Han, J. (2022). Construction of rice protein-based meat analogues by extruding process: Effect of substitution of soy protein with rice protein on dynamic energy, appearance, physicochemical, and textural properties of meat analogues. *Food Research International, 161*, Article 111840.

Lee, J.-S., Oh, H., Choi, I., Yoon, C. S., & Han, J. (2022a). Physico-chemical characteristics of rice protein-based novel textured vegetable proteins as meat analogues produced by low-moisture extrusion cooking technology. *Lwt, 157*, Article 113056.

Lin, Q., Pan, L., Deng, N., Sang, M., Cai, K., Chen, C., et al. (2022). Protein digestibility of textured-wheat-protein (TWP) -based meat analogues: (I) effects of fibrous structure. *Food Hydrocolloids, 130*, Article 107694. https://doi.org/10.1016/j.foodhyd.2022.107694

Ma, R., Jin, Z., Wang, F., & Tian, Y. (2022). Contribution of starch to the flavor of rice-based instant foods. *Critical Reviews in Food Science and Nutrition, 62*(31), 8577–8588.

Meng, A., Chen, F., Zhao, D., Wei, Y., & Zhang, B. (2022). Identifying changes in soybean protein properties during high-moisture extrusion processing using dead-stop operation. *Food Chemistry, 395*, Article 133599. https://doi.org/10.1016/j.foodchem.2022.133599

Omura, M. H., de Oliveira, A. P. H., de Souza Soares, L., dos Reis Coimbra, J. S., de Barros, F. A. R., Vidigal, M. C. T. R., … de Oliveira, E. B. (2021). Effects of protein concentration during ultrasonic processing on physicochemical properties and techno-functionality of plant food proteins. *Food Hydrocolloids, 113*, Article 106457.

Rai, A., Sharma, V. K., Sharma, M., Singh, S. M., Singh, B. N., Pandey, A., et al. (2023). A global perspective on a new paradigm shift in bio-based meat alternatives for healthy diet. *Food Research International, 169*, Article 112935.

Samard, S., Maung, T.-T., Gu, B.-Y., Kim, M.-H., & Ryu, G.-H. (2021). Influences of extrusion parameters on physicochemical properties of textured vegetable proteins and its meatless burger patty. *Food Science and Biotechnology, 30*, 395–403. https://doi.org/10.1007/s10068-021-00879-y

Samard, S., & Ryu, G. H. (2019). A comparison of physicochemical characteristics, texture, and structure of meat analogue and meats. *Journal of the Science of Food and Agriculture, 99*(6), 2708–2715. https://doi.org/10.1002/jsfa.9438

Shevkani, K., Singh, N., Chen, Y., Kaur, A., & Yu, L. (2019). Pulse proteins: Secondary structure, functionality and applications. *Journal of Food Science and Technology, 56*, 2787–2798.

Singh, M., Trivedi, N., Enamala, M. K., Kuppam, C., Parikh, P., Nikolova, M. P., et al. (2021). Plant-based meat analogue (PBMA) as a sustainable food: A concise review. *European Food Research and Technology, 247*(10), 2499–2526. https://doi.org/10.1007/s00217-021-03810-1

Sun, C., Ge, J., He, J., Gan, R., & Fang, Y. (2021). Processing, quality, safety, and acceptance of meat analogue products. *Engineering, 7*(5), 674–678.

Tolstoguzov, V. B. (1993). Thermoplastic extrusion—the mechanism of the formation of extrudate structure and properties. *Journal of the American Oil Chemists' Society, 70*(4), 417–424. https://doi.org/10.1007/BF02552717

Van Der Sman, R., & Van Der Goot, A. (2023). Hypotheses concerning structuring of extruded meat analogs. *Current Research in Food Science, 6*, Article 100510. https://doi.org/10.1016/j.crfs.2023.100510

Wang, T., Kaur, L., Furuhata, Y., Aoyama, H., & Singh, J. (2022). 3D printing of textured soft hybrid meat analogues. *Foods, 11*(3). https://doi.org/10.3390/foods11030478

Wang, H., van den Berg, F. W. J., Zhang, W., Czaja, T. P., Zhang, L., Jespersen, B. M., et al. (2022). Differences in physicochemical properties of high-moisture extrudates prepared from soy and pea protein isolates. *Food Hydrocolloids, 128*. https://doi.org/10.1016/j.foodhyd.2022.107540

Wittek, P., Karbstein, H. P., & Emin, M. A. (2021). Blending proteins in high moisture extrusion to design meat analogues: Rheological properties, morphology development and product properties. *Foods, 10*(7), 1509. https://doi.org/10.3390/foods10071509

Xiao, Z., Jiang, R., Huo, J., Wang, H., Li, H., Su, S., et al. (2022). Rice bran meat analogs: Relationship between extrusion parameters, apparent properties and secondary structures. *Lwt, 163*, Article 113535. https://doi.org/10.1016/j.lwt.2022.113535

Xia, S., Shen, S., Song, J., Li, K., Qin, X., Jiang, X., … Xue, Y. (2023). Physicochemical and structural properties of meat analogues from yeast and soy protein prepared via high-moisture extrusion. *Food Chemistry, 402*, 134265.

Xia, S., Xue, Y., Xue, C., Jiang, X., & Li, J. (2022). Structural and rheological properties of meat analogues from Haematococcus pluvialis residue-pea protein by high moisture extrusion. *LWT, 154*, Article 112756. https://doi.org/10.1016/j.lwt.2021.112756

Yuliarti, O., Kiat Kovis, T. J., & Yi, N. J. (2021). Structuring the meat analogue by using plant-based derived composites. *Journal of Food Engineering, 288*. https://doi.org/10.1016/j.jfoodeng.2020.110138

Zahari, I., Ferawati, F., Helstad, A., Ahlström, C., Östbring, K., Rayner, M., et al. (2020). Development of high-moisture meat analogues with hemp and soy protein using extrusion cooking. *Foods, 9*(6), 772. https://doi.org/10.3390/foods9060772

Zhang, B., Kang, X., Cheng, Y., Cui, B., & Abd El-Aty, A. M. (2022). Impact of high moisture contents on the structure and functional properties of pea protein isolate during extrusion. *Food Hydrocolloids, 127*. https://doi.org/10.1016/j.foodhyd.2022.107508

Zhang, J., Liu, L., Liu, H., Yoon, A., Rizvi, S. S., & Wang, Q. (2019). Changes in conformation and quality of vegetable protein during texturization process by extrusion. *Critical Reviews in Food Science and Nutrition, 59*(20), 3267–3280. https://doi.org/10.1080/10408398.2018.1487383